Journal of Indian Geomorphology
Volume 9, 2021 ● ISSN 2320-0731
Indian Institute of Geomorphologists (IGI)

Geomorphic Evolution of Chalakudy River Basin, South Western Ghat, India: Insights from Drainage Morphometric Indices

A. U. Anish[1], K. R. Baiju[2], G. Girish[3], V. Ambili[4], K. P. Thrivikramji[5]
[1]*Department of Geology, Government College Kottayam, Kerala 686013*
[2]*School of Environmental Sciences, Mahatma Gandhi University, Kottayam, Kerala 686560*
[3]*Centre for Water Resource Development and Management, Kozhikode, Kerala 673 571*
[4]*Geological Survey of India, Marine & Coastal Survey Division, Marripalem, Visakhapatnam, Andhra Pradesh 530007*
[5]*Centre for Environment and Development, Thiruvanthapuram, Kerala 695010*
E-mail: anishgold@gmail.com(Corresponding author)

Abstract: *The geomorphic evolutionary characteristics and the stages of fluvial landscape evolution of the Chalakudy River Basin (CRB), South Western Ghats, based on hypsometry from SRTM DEM data and Survey of India (SOI) topo-maps has been attempted in the present study. The relative tectonic activity index (Iat) has been interpreted from the drainage morphometric parameters; viz. stream gradient index, basin asymmetry factor, hypsometric integral, percent basin asymmetry factor, basin length to width ratio, valley floor width to valley height ratio and mountain front sinuosity. The stages of geomorphic evolution and extent of the 'subdued' topography of the sub-basins are interpreted from the attributes of hypsometric curve (HC), viz. head and toe values of HC, coordinates of slope inflection points of HC and hypsometric integral value. Iat is moderate - low for sub-basins of CRB and the sub-basins exhibit mature stage of geomorphic evolution. It is proposed that the sub-basins of CRB have evolved through hill slope retreat influenced by diffusive process.*

Key words: Morphometry, Relative tectonic activity index (Iat), Hypsometry, Geomorphic evolution.

Introduction

River basins evolve under the influence of geologic, tectonic and climatic factors operating over a long span of time (Strahler, 1952, 1956). The progress of evolution of fluvial landform through young, mature and old age or monadnock stages in the sub-basins of a drainage system can be reliably deduced from the hypsometry or the area-elevation relationship of a drainage basin (Schumm, 1956; Strahler, 1952, 1956; Sinha Roy, 2002). Two key competitive factors involved in the fluvial landscape development are the tectonic uplift and down-wasting due to erosion (Sinha Roy, 2002). Specifically, geomorphic evolution and drainage network configuration depend on the active tectonic factors, which are often modified by various denudation processes operating in the drainage basin (Duvall, and Kirby, 2004). The active tectonic responses within the sub-basins of a drainage basin can be evaluated using quantitative analysis of geomorphic indices and the history of low magnitude earthquakes (Bull and McFadden, 1977; El Hamdouni *et al.*, 2008; Keller and

Pinter, 1996). El Hamdouni *et al.*, (2008) proposed a method of integratingseveral geomorphic indices to a single construct, to picture the active tectonic response of Sierra Nevada (southern Spain) terrain. The scheme, proposed by El Hamdouni *et al.* (2008) has been used to determine the relative tectonic activity index (Iat) of Chalakudy river basin (CRB), in south central Kerala. The geomorphic evolutionary stages of the CRB, based on hypsometric analysis are presented in this research paper. In this study, estimation, analysis and integration of morphometric indices have been carried out from input of vectorised Survey of India (SoI) topographical maps, SRTM-DEM data and ASTERGDEM data, using geospatial technology.

Regional setting

The CRB (location: 10°15´N–10°35´N and 76°15´E–76°55´E; area: 1448.0 km^2), falls in the districts of Thrissur, Ernakulam, and Palakkad of Kerala, and partly in Coimbatore district (329.6 km^2) of Tamil Nadu. The river originates in the Anamalai hills of the Western Ghats (WG) flowing westward for ~144 km, before it joins the Periyar river. The river flows over a crystalline basement of metamorphic/ igneous rocks, creating geomorphological features like waterfalls, cascades, rapids, meanders, stabilised channel-islands, terraces, sandbars etc. The major extent of CRB is covered by densest evergreen reserve forest. Six major tributaries of CRB, such as Sholaiar, Parambikolam Ar, Kuriyarkuty Ar, Karapara Ar, Kannankuzhy Ar and Anakkayam Ar, make it a 7th order river before joining Periyar river (Fig.1). The river originates from a terrain of peaks and ridges (altitude: >1800 m) initially, then flows through highland (altitude: 1800–600 m), midland (altitude: 600–300 m) and lowland (300–0 m) depicting the major physiographic divisions of Kerala (Fig. 1).

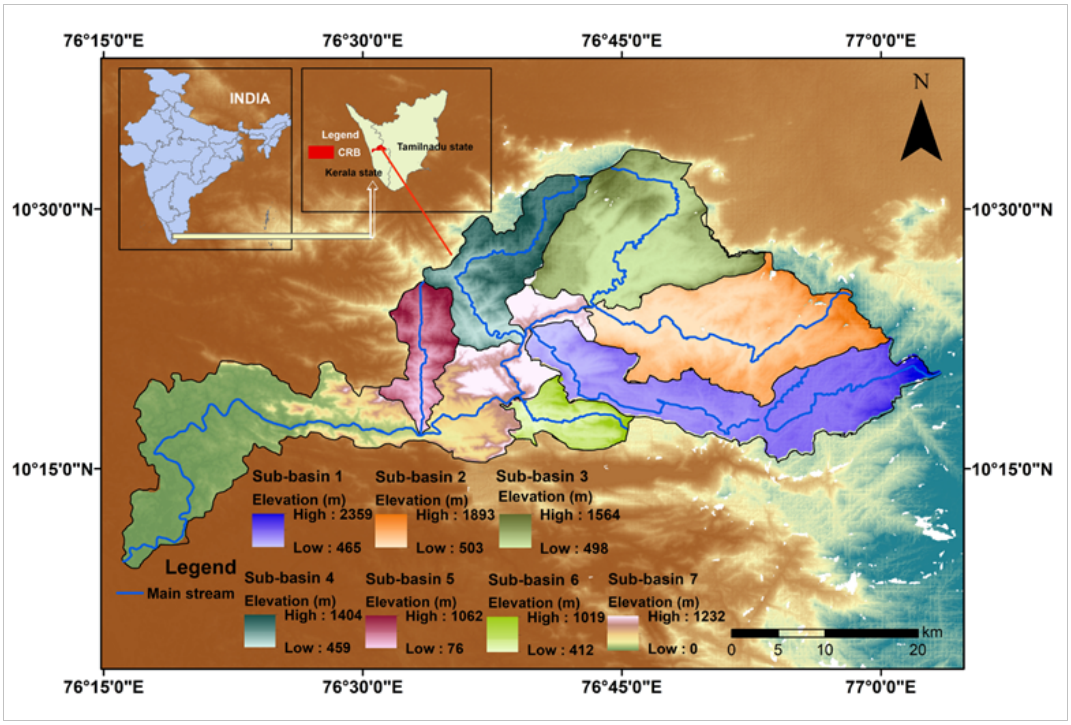

Figure 1. Location map of the study area

The study area forms part of the southern granulite terrain characterised by Proterozoic crystalline rocks, Charnockites and associated gneisses (hornblende biotite gneiss and biotite gneiss) and intrusions of granites, syenites, and gabbro (Soman, 2002; Babu *et al.*, 2012). CRB is traversed by NW-SE trending dykes (pegmatites, gabbro, dolerite) linked to Indo-Madagascar-Seychelles rifting and later continental extension, superimposed on Dharwar trend. The ages of these mafic dykes vary from early Cretaceous to late Cretaceous (Ajaya kumar and Rajendran, 2017). The CRB is traversed by numerous prominent NNW-SSE trending structural lineaments extending from the Periyar fault (Singh, *et al.*, 2016) along with sub-numerous NNE-SSW and E-W trending minor lineaments (Fig. 2).

Materials and methods

In this research paper, geomorphometric indices of CRB for each of its sub-basins, such as Sholaiar (1), Parambikolam (2), Kuriarkutty (3), Karapara (4), Kannankuzhy (5), Anakayam (6) and the main stream (7) respectively have been analysed. From the georeferenced Survey of India open series topographical-maps (viz., 58B/7, 58B/8, 58B/11, 58B/13/, 58 B/15, 58F/3 of 1: 50,000 scale), sub-basin boundaries and drainage data are delineated in vector data for and have been rasterised for further analysis.

Integration and interpretation of morphometric data and hypsometric characterisation form the major part of the study. Drainage basin area, basin length to basin width ratio (*Bs*) and basin mean width ratio are determined from the vectorised data. For constructing hypsometric curves, computing hypsometric integral (*Ea*) and for TIN map preparation SRTM data (3 Arc second or 90 m) has been used. Lineament traces of CRB are mapped from Aster GDEM

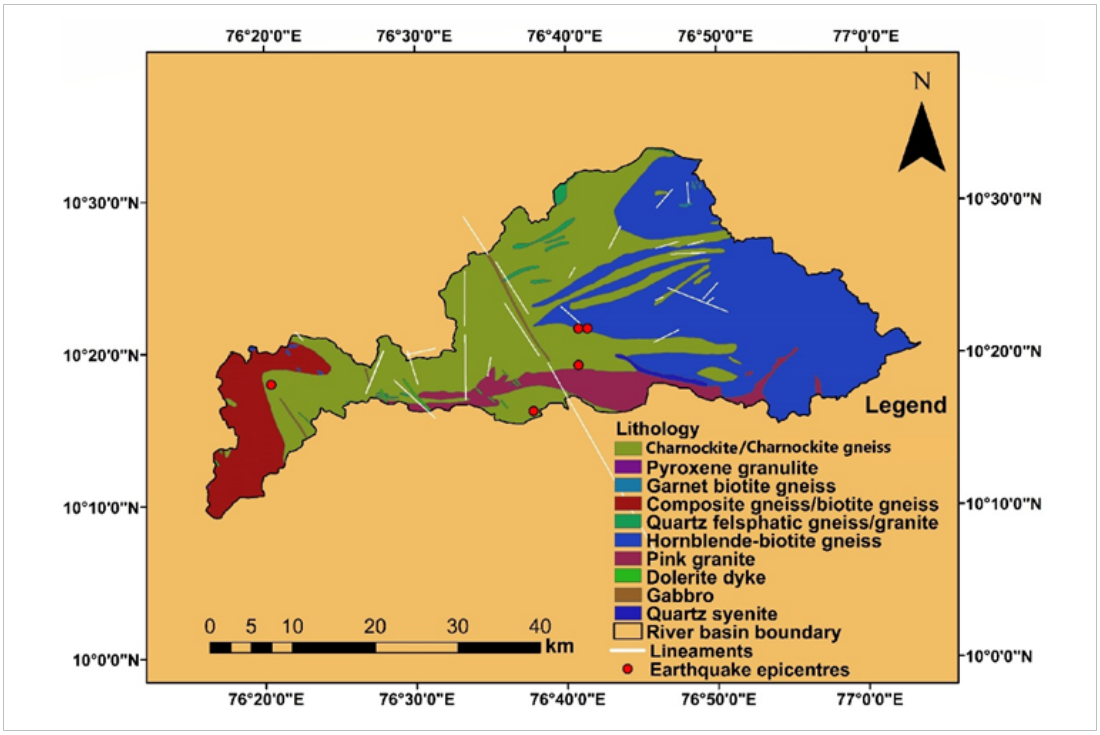

Figure 2. Lithologic map with lineament traces derived from Aster GDEM data (updated with lineament data of CRB in bhuvan.nrsc.gov.in) and recent earthquake epicenters of CRB.

Table 1: Geomorphic indices and their computation

Morphometric parameters and acronym	Equation	Description	Inference that can be drawn from the parameter	References
Basin asymmetry factor (BAF)	BAF = Ar/At x 100	Ar = drainage area on the downstream right-hand side of the main drainage line and At = total drainage area.	BAF factor expresses the lateral tilting of the basin. BAF of ~50 indicates no or little tilt, > 50 indicates tilt towards left and <50 represents tilt towards right.	(Hare and Gardner, 1985; Cox, 1994; El Hamdouni *et al.*, 2008; Keller and Pinter, 2002; Ozkaymak and Sozbilir, 2012)
Percentage of basin asymmetry factor (PBAF)	PBAF=(ALS/At) x 100, Where ALS is the area of larger side of the main stream of basin and At is the total basin area.	Ratio of the area of the larger portion of the basin to the total area of the basin	Degree of tilting of basins can be interpreted. Values of PBAF significantly greater than 50 (close to 100) suggest the high percent of basin asymmetry.	(Bahrami, 2013)
Transverse topography Symmetry (T)	T =Da/Dd	Dais that distance from the basin midline to the channel and Dd is the distance from the midline to the drainage divide.	Symmetry characteristics of the basin can be interpreted.	(Cox, 1994)
Valley floor width to valley height ratio (*Vf*)	*Vf* = 2 Vfw/ [(Erd-Esc) + (Eld- Esc)]	Vfwis the valley floor width of the mainstream channel, Erd, Eld and Esc are the elevations of the right, left drainage divide, and valley floor of the sub-basin respectively	Valley floor width to valley height ratio defines the shape of valley profile signifying the driving forces in its development.	(Bull and Mcfadden, 1977; Dehbozorgi *et al.*, 2010)
Mountain front sinuosity factor (Smf)	Smf = Lmf/Ls	Lmf is the length of the mountain front along its foot and Lsis the straight-line length of the mountain front	Straight mountain fronts are intimately related with faults and irregular fronts results from active erosion	(Bull and McFadden, 1977; Keller and Pinter, 2002; Dar *et al.*, 2013; Ahamed *et al.*, 2018)
Stream gradient index $SL_{segment}$	$SL_{segment}$ = (H) Lx L	His difference in elevation between two points along the mainstream channel (H_elv - L_elv), L is the horizontal distance between points of higher elevation (H _elv) and lower elevation (L _elv) in the stream segment and L is the total length measured from the drainage divide to the midpoint of the stream segment where the measurement is made.	Topographic characteristics can be interpreted.	(Hack, 1973)

data (1 Arc secondor 30 m) and a data updating was done in Bhuvan (bhuvan.nrsc.gov.in) of Indian Space Research Organisation (ISRO).

El Hamdouni *et al.* (2008) proposed a method for calculating the relative tectonic activity index (*Iat*) using morphometric parameters such as stream gradient index (*SL*), drainage basin asymmetry (*Af*), hypsometric integral (*Ea*), ratio of valley floor width to valley floor height (*Vf*), and mountain front sinuosity (*Smf*) (Table 1). *Vf* of each sub-basin is computed from the average value of 5 cross profiles of main valley. Processing of SRTM data under 3D analyst tool was used for the generation of cross profiles.The *Smf* and *Bs* values were derived from SRTM data. Hypsometry, an estimate of the distribution of the surface area of a landmass at different elevations (Strahler, 1952), is a proxy to delineate tectonically active and inactive areas of the basin, to unravel the geomorphic stages of landscape evolution (Lifton and Chase, 1992).

The hypsometric curve (*HC*) is a plot of the relative area against relative height defining the proportion of land area that exists at various elevations above or below a datum (Strahler, 1952; Fairbridge, 1968). Area below the curve (*Ea*) is equivalent to the volume of rocks remaining in the drainage basin (Strahler, 1952; Pike and Wilson, 1971; Chen *et al.*, 2003; Panek, 2004).

HC plot (Strahler, 1964) representing sub-basin elevation (h) normalised against the maximum height (*H*) and abscissa corresponds to area (a), normalised against total area (A) of the sub-basin is used for interpreting the geomorphic evolution of CRB. Evolutionary stages of the sub-basins can be deduced from the shape of hypsometric curve, head and toe values, coordinates of slope inflection points and hypsometric integral (Strahler, 1952, 1964; Pike and Wilson, 1971; Willgoose and Hancock, 1998; Sinha Roy, 2002; Walcot and Summerfield, 2008; Dash *et al.*, 2014). The statistical characterisation of the drainage morphometric parameters were deduced from the Pearson's correlation matrix.

Results and discussion

Drainage morphometry

Organisation of drainage network and its progress are under the control of lithological characteristics, tectonic controls and climatic zone operating in the drainage basin. The morphologic aspects and topography of a drainage basin influence a number of hydrologic processes operating in the basin (Kale and Gupta, 2001; Gadre, 2006). Analysis of basin shape parameters, longitudinal profile and anomalies in hypsometry can dictate the neotectonic/tectonic activities in the drainage basin (Deffontaines *et al.*, 1992; Ambili and Narayana, 2014; Thomas and Prasanna kumar, 2017). The basin morphometry is described in terms of basin shape parameters - *Bs, BAF, PBAF, T* and *Smf*.

Basin length to width ratio or aspect ratio (*Bs*)

El Hamdouni *et al.* (2008), Mahmood and Gloaguen (2012), and Bahrami, (2013) have proposed that drainage basin is narrow and elongated particularly in the head portion of tectonically active young drainage basins, and *Bs* is an important parameter for describing the role of tectonics in shaping the basins. Though tectonics modifies the basin characteristics, yet dies off over time, the elongated younger drainage basins near the mountain front transform to circular basins (Bull and McFadden, 1977). The drainage basins with *Bs* value >4, denote the role of tectonics in shaping the fluvial landscape. *Bs* values in the range of 3 to 4, characterise drainage basins of slight-active-tectonics and values <3 are near circular plan view and hence are tectonically inactive (El Hamdouni *et al.*, 2008; Ahmad *et al.*, 2018). *Bs* value of

5.23 for sub-basin 1 is suggestive of tectonic imprint or response, as other sub-basin does not show tectonic imprints based on *Bs* value (Table 2).

Table 2: *Bs*, *PAF*, *PBAF*, *T* values of CRB

Sub-basin	Bs	BAF	PBAF	T
Sub-basin 1	5.23	58.15	0.58	0.29
Sub-basin 2	1.99	45.60	0.54	0.33
Sub-basin 3	0.85	53.47	0.53	0.32
Sub-basin 4	2.54	53.41	0.53	0.28
Sub-basin 5	2.39	47.13	0.53	0.27
Sub-basin 6	2.10	40.70	0.59	0.37
Sub-basin 7	3.64	54.57	0.55	0.54

Basin asymmetry factor (*BAF*)

BAF values of CRB indicate that the sub-basin 1 has a moderate NE tilt, while the sub-basin 6 tilts NW. However, the (*PBAF*) values show moderate tilt for sub-basins 1 and 6 (Table 2). For a perfectly symmetric basin, (*T*) value ought to be zero and the asymmetry of the basin increases if the value approaches 1.0. Average T values of the CRB sub-basins is 0.3 (Table 2), implying near symmetry and the sub-basin 7 reports a maximum of 0.54.

Valley floor width to valley height ratio (*Vf*)

The *Vf* value signifies the valley shape and the processes responsible for its development.The 'U' shaped valleys are created by the active lateral erosion and 'V' shaped valleys are created by active vertical incision in response to baselevel changes due to upliftment of the terrain. Higher *Vf* values surrogate high incision rate related to tectonic processes (El Hamdouni *et al.*, 2008). *Vf* values >1.0 characterises 'V' shaped valleys, created by incision forced by upliftment and values between 1.0 and 1.5 are indicative of basins with moderate tectonic imprints, while values >1.5 are suggestive of 'U' shaped valleys that evolved through lateral erosion (Bull and McFadden, 1977; Keller and Pinter, 2002; Ahmad *et al.*, 2018). The *Vf* of 1.34, 1.40 and 1.49 for sub-basins 5, 2 and 1 indicate moderate tectonic imprint, while *Vf* of 2.07, 2.57, 2.92, 4.11 for sub-basins 6, 3, 4, and 7 manifest 'U' shaped crossprofile, developed due to active erosion and/ or anthropogenic interference (Table 3). The high *Vf* value of sub-basin 7 is consequent to the high discharge of water through the main stream channel.

Mountain front sinuosity *(Smf)*

The shape of the mountain front is a key to the processes responsible for its development. Higher value of *Smf* suggests irregular mountain fronts resulting from erosion and lower *Smf* values associate themselves with straight mountain front which are mostly due to fault tectonics (Bull and McFadden, 1977; Keller and Pinter, 1996). Bull and McFadden (1977) proposed that *Smf* values ranging from 1-1.6 are characteristic of active mountain fronts; values between 1.4–3.0 characterise less active mountain fronts, whereas values

Table 3: SL, PBAF-50, Ea, Bs, Vf, Smf value and Iat of the classes of sub-basins of CRB. Ranks are assigned to each parameter — SL class: 500> = 1 , 500 – 300 = 2, <300 = 3, Ea class: 0.5> = 1, 0.5 – 0.35 = 2, <0.35 = 3, PBAF class: 9.0> = 1, 9 – 4.5 = 2, <4.5 = 3, Smf class: 1.0 – 1.4 = 1, 1.4 – 3.0 = 2, 3> = 3, Vf class: <1.0 = 1, 1.0 – 1.5 =2, 1.5> = 3. Iat class: 1.5 – 2.0 = Class 1 HT, 2.0 – 2.5 = Class 2 MT, above 2.5 = Class 3 LT, where HT, MT and LT refer to high, moderate and low relative tectonic indices.

Sub-basin	SL	PBAF-50	Ea	Bs	Vf	Smf	Weightage of Iat (S)	Value of Iat (S/n)	Iat Class
Sub- basin 1	870	8.15	0.47	5.23	1.49	1.27			
Class	1	2	2	1	2	1	9	1.5	II HT
Sub- basin 2	452.1	4.4	0.45	1.99	1.4	1.46			
Class	2	3	2	2	2	2	13	2.17	III MT
Sub- basin 3	263.3	3.47	0.45	0.85	2.57	1.63			
Class	3	3	2	3	3	2	16	2.66	III LT
Sub- basin 4	364.4	3.41	0.47	2.54	2.92	1.48			
Class	2	3	2	2	3	2	14	2.33	III MT
Sub- basin 5	227.4	2.86	0.48	2.39	1.34	1.42			
Class	3	3	2	2	2	2	14	2.33	III MT
Sub- basin 6	158.5	9.3	0.43	2.1	2.07	1.43			
Class	3	1	2	2	3	2	13	2.16	III MT
Sub- basin 7	64.2	4.57	0.41	3.64	4.11	1.62			
Class	3	2	2	1	3	2	13	2.17	III MT

>3.0 reflect inactive mountain fronts (Dar *et al.*, 2012; Ahmad *et al.*, 2018). *Smf* values of sub basins of CRB are calculated for 32 locations and the averages for 6 sub basins lie between 1.3 and 1.6 (Table 3). But majority of *Smf* values in CRB fall in the 1.4 -3.0 class of the mountain front sinuosity classification by Bull and McFadden (1977) implying less active, mountain fronts in the basin.

Basin relief characteristics

The occurrence of latent tectonic imprints in stream channel like bed rock floor, cascades and other variables contributing to the drainage (basin) modifications, can be easily deciphered from the analysis of relief attributes such as longitudinal profile, stream gradient index and hypsometric analysis (Duval *et al.*, 2004; Martinez *et al.*, 2011; Doranti Tiritan *et al.*, 2014).

Longitudinal profile

Longitudinal profile is the manifestation of the channel gradient and provides clues to the nature of underlying materials and insights to the operation of geological processes and geomorphologic evolutionary history of the drainage basin (Hack, 1973; Ouchi,

1985; Schumm, 1956; Ambili and Narayana, 2014). Longitudinal profile of the sub-basin 1, is characterised by convex segments, marked as knick points at 1800 m, 1000 m and 700 m. The sub-basin II shows convex segments at 1400 m and 1100 m. Sub-basins 3 and 6 show concave upward longitudinal profiles, characteristic of a graded stream. Perturbations in sub-basin 4, are indicated in the long profile at elevations of 900 m, 600 m and 500 m. Sub-basin 5 shows the anomaly in the smooth longitudinal profile at 500 and 420 m respectively. Sub-basin 6 shows knick points at 500 m and 200 m (Fig.3 a–d).

STREAM GRADIENT INDEX (SL)

SL relates the slope of a drainage system to its length at a specific region of the drainage basin and act as a relative gauge that indicates the competence and capacity of a drainage system. It reflects the channel characteristics that resist flow (Hack, 1973). The variation in SL value along the downstream segments serves as a proxy for identifying difference in bedrock characteristics signifying the influence of tectonics/ lithology in molding fluvial landscapes. The average SL values of the sub-basins determined down the main stream channel ranges from 64 to 870 (Table 3). The sub-basin 1 shows SL values >500 and the sub-basins 2 and 4 shows value >300. The sub-basins 3 and 5 are characterised by SL value >200 and sub-basin 7 shows SL

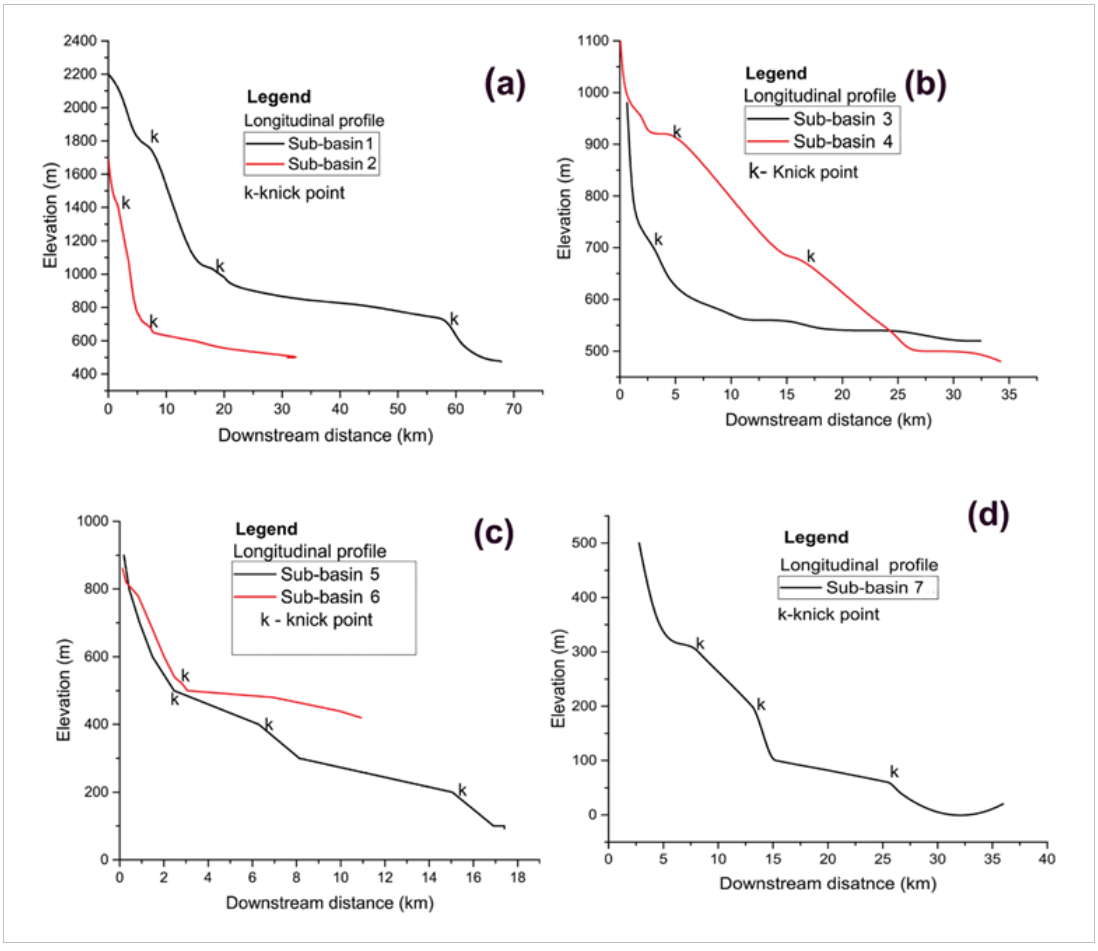

Figure 3 a–d. Longitudinal profile of sub- basins of CRB

values <100.

Relative tectonic activity index (Iat)

The relative tectonic activity index (*Iat*) of sub-basins of CRB is computed from parameters of *SL, PBAF, Ea, Bs*, *Vf* and *Smf*. To estimate *Iat*, the drainage morphometric parameters are grouped into classes (Table 3). SL is grouped into three classes, viz. SL > 500 (Class 1), SL between 500-300 (Class 2) and SL <300 (Class 3) (Dehbozorgi *et al.*, 2010). The difference between calculated PBAF value and neutral value (i.e. 50), ranges from 2.86–9.3, are also grouped into three classes 1, 2 and 3 respectively for PBAF >9, 9< PBAF >4.5 and PBAF <4.5. The *Ea* values are classed into 1, 2 and 3 respectively as: *Ea* ≥0.5, *Ea* <0.5 *Ea* > 0.35, *Ea* <0.35. Besides, *Bs* values are classified into 1, 2 and 3as: *Bs* >3, *Bs* 3 >*Bs* >2, *Bs* <2 respectively. *Vf* values greater than 1.0 is reflective of active tectonic characteristics of the basin (Class 1), values between 1.0 and 1.5 represent basins with moderate tectonic imprints (Class 2) and values above 1.5 implies (Class 3). *Smf* values are classed into three catagories – Classes 1, 2 and 3 with values 1.0–1.4, 1.4–3.0 and >3 respectively (Ahmad *et al.*, 2018).

The average of the different classes of geomorphic indices (S/n), called the *Iat*, are obtained from the indices of SL, PBAF, *Ea*, *Bs*, *Vf*, *Smf* and are grouped into four classes (Table 3). Class 1 falls under very high tectonic activity with S/n values between 1 and 1.5; Class 2 (high tectonic activity) having S/n values >1.5 but <2; Class 3 of moderately active tectonics with S/n values >2 but <2.5 and lastly Class IV with low tectonic activity and having S/n >2.5 (El Hamdouni *et al.*, 2008).

Integration of geomorphic indices to infer the relative tectonic activity index (*Iat*), shows that sub-basins (except sub-basin 1 and 3) belongs to Class 3 of moderate tectonic activity response. Low tectonic index is reflected by sub-basin 3. Sub-basin 1 belongs to Class 2, reflecting its relatively high tectonic activity response among other sub-basins, evidenced by its elongated basin shape and asymmetry characteristics.

Hypsometry

The shape of the *HC* and the value of *Ea* reflect the influences of lithology and extent of erosion in the development of fluvial landscapes (Farhan *et al.*, 2016)

Hypsometric curve *(HC)*

HC is the elevation frequency distribution, which is directly related to the denudation and the relative slope of the basin. *HC* translates from convex to concave as the drainage basin progresses from youthful to old age stages of geomorphic evolution (Fig.4).

'*Ea*' denotes the hypsometric integral value refers to the area under *HC* expressed

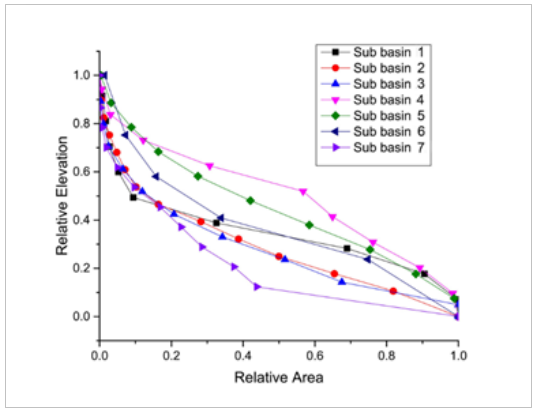

Figure 4. Hypsometric curves of sub-basins of CRB

in percentage of area PQRS. 'Eh' is the maximum concavity of *HC* measured from the line P-R joining the head and toe elevations of the sub-basin. Eh coincides at 'I' the slope inflection point referring to the shift from either concave to convex trend of *HC* or vice–versa. The value of 'Eh' is positive (*HC* below the line P-R) for mature and old stage landforms and negative (*HC* above P-R) for

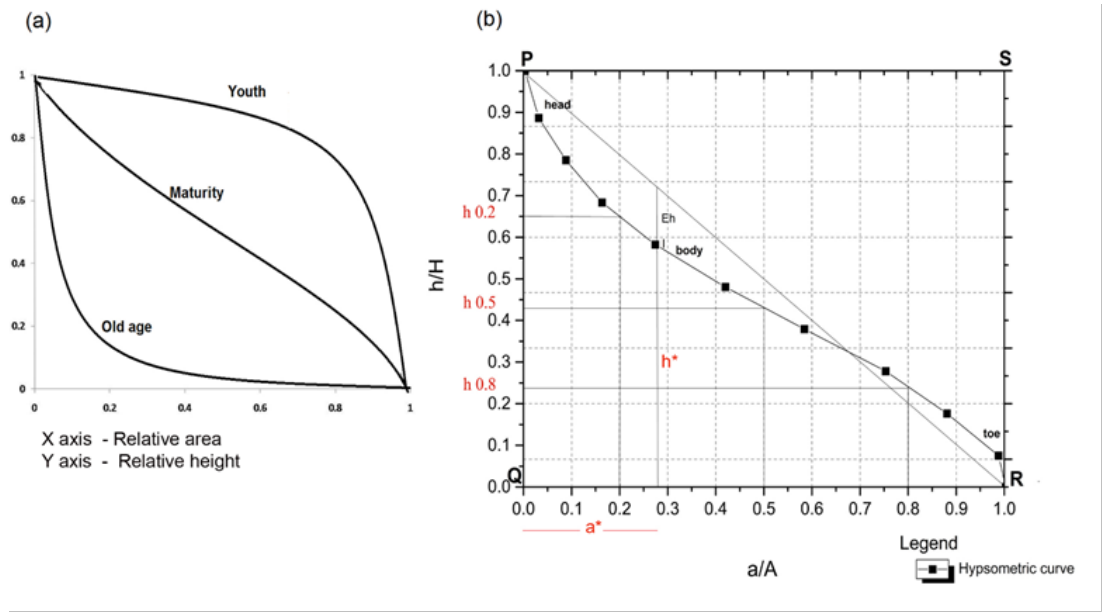

Figure 5 (a). Hypsometric curve shape and geomorphic evolution stages (after Strahler, 1964); (b) Depiction of hypsometric curve (*HC*) parameters, relative elevation (h/H) and relative area (a/A) on vertical and horizontal axes. Parts of *HC*: head, body and toe. The downward concave segment of the *HC*, located at right hand side of the observer is called 'toe' and the upward concave part of *HC*, at the left hand side of the observer is called 'head'. The segment in between toe and head is called 'body'.

immature/young landforms. The co-ordinates of slope inflection point 'I' on ordinate and abscissa of *HC* plot are given by h* and a* respectively. H (0.2), h (0.5), h (0.8), h (0.9) are the normalised heights of the *HC* at 20, 50, 80, 90 percentages respectively of the sub-basins. The h* and a* values signifies the erosional characteristics of the sub-basin, lower the value of a*, greater will be the extent of subdued topography and lower h* value reflects the extent of the degree of peneplanation (after Sinha Roy., 2002; Fig. 5)

Hypsometric integral (*Ea*)

Area under the *HC* signifies the mass of rocks that resisted the process of erosion and can be quantitatively expressed as (*Ea*), which theoretically varies from 0.0 to 1.0. For e.g., *Ea* values >0.65 indicate a youthful stage, between 0.35 and 0.65 mature stage, and < 0.35 characterises the monadnock stage (Strahler, 1952; Sedrette *et al.*, 2016). How importantly tectonics, climate, and lithologic control on drainage basin development, is inferable from the shape of hypsometric curve and the *Ea* values (Willgoose and Hancock, 1998; Pérez-Peña *et al.*, 2009; Willett, *et al.*, 2014). The sub-basins of CRB are divided into third order watersheds and *Ea* values are calculated.

Hypsometric characterisation

Relief characteristics of the terrain can be fairly reliably deduced from the analysis of *HC* and *Ea* values (Anderson and Anderson, 2010). There exists a strong relationship between relief and area, and provides a window to the landform process and hence geomorphic evolution. So, the detailed analysis of *HC* and *Ea* clearly defines the young, mature equilibrium stage and monadnock stage of geomorphic evolution (Strahler, 1952) (Fig. 5a). Type II *HC* curve (Fig. 5b) with relative area a/A on abscissa and relative elevation h/H on ordinate, is divisible into different segments viz. head, toe and

Table 4: Eh, Ea , a* and h*, Av. Rbvalues of CRB

Sub-basin	Area (km^2)	Height of Hypsometric curve						Coordinates of (I)		
		Ea	At 0.2	At 0.5	At 0.8	At 0.9	Eh	a*	h*	Av: Rb
Sub-basin 1	259.14	0.47	0.45	0.34	0.23	0.18	0.39	0.08	0.52	5.21
Sub-basin 2	255.04	0.45	0.44	0.25	0.11	0.08	0.43	0.11	0.48	4.13
Sub-basin 3	232.67	0.45	0.42	0.25	0.11	0.08	0.46	0.18	0.45	3.83
Sub-basin 4	133.52	0.47	0.68	0.55	0.28	0.19	0.10	0.03	0.84	4.19
Sub-basin 5	72.05	0.48	0.65	0.43	0.24	0.16	0.15	0.16	0.68	4.03
Sub-basin 6	58.64	0.43	0.54	0.34	0.20	0.10	0.27	0.29	0.44	4.71
Sub-basin 7	436.94	0.41	0.41	0.11	0.04	0.02	0.41	0.06	0.59	4.45

body (Willgoose and Hancock, 1998; Sinha Roy, 2002). The normalised elevation value (h) of the *HC* curve at ordinate corresponding to values of relative area, i.e., 0.2, 0.5, 0.8 and 0.9 on the abscissa are calculated for seven sub-basins of CRB. The slope inflection points at *HC* are also determined and corresponding values of relative area and elevation on abscissa and ordinates are represented as a* and h* (Table 4). The *Ea* has profound control on the shape of *HC* (Sinha Roy, 2002) and *Ea* values classes $0< Ea <0.35$, $0.35 <Ea <0.65$ and $0.65 <Ea <1$, signify the old, mature and youth stages of geomorphic evolution of a drainage basin.

Shape of hypsometric curve (*HC*)

Shape of hypsometric curve is a signature of the stages of evolution of the landforms (Troeh, 1965, Sinha Roy, 2002). Standard *HC*, viz., Type-1, Type-2, Type 3, Type 4 are explained by Willgoose *et al.* (1991) and Willgoose (1994) (Fig. 5). *HC* shapes of CRB, fall under two classes, viz., *HC* with profound concavity (concave-up with water gathering slope) in the head-ward part and extending toward its toe or lower reaches or Type 1, and *HC* with concavity in the upper part and slight convexity (concave-up water-spreading slope) toward the lower part or Type 4 (Fig.6). It is evident from the figure that the sub-basin 7 belongs to Type 1 standard curve and all the other sub-basins belong to Type 4. Type 1-*HC* indicates the dominance of fluvial processes during the geomorphic evolution. Type 4-*HC* reflects the earlier stages of fluvial processes and later episodes of diffusive processes in geomorphic evolution and mass accumulation towards downstream, which in turn results in the increase of elevation toward the mouth of the catchment.

Type 4 evolved by initial fluvial process modified further by diffusive processes in the downstream segments and resultant mass accumulation towards mouth. Type 2 and *HC* signature represents sub-basins where fluvial process are superimposed on an older landform formed by diffusive process. Strahler classified geomorphic evolutionary stage progression from youth to old age stage through Type 3 to Type 1 through Type 2 and Type 4. Type 4 representing mature stage is the general *HC* signature shown by sub-basins of CRB (Fig. 6).

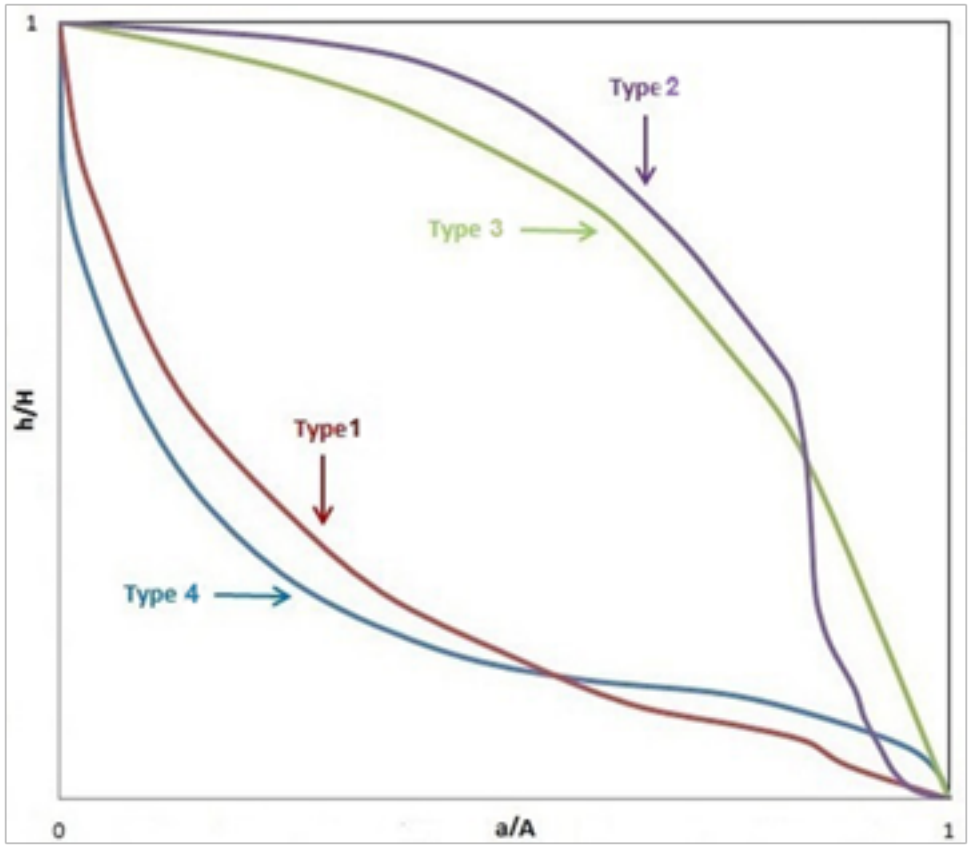

Figure 6. Standard hypsometric curve types (after Willgoose, ***et al.***, 1991, Willgoose, 1994). Type 1 is characteristic of basins evolved through fluvial processes and Type 2 by diffusive process.

Head and toe values of *HC*

Head value of *HC* reflects the extent of diffusive process at the head-ward part of the drainage basin, whereas the toe value reflects the accumulation of denudated materials towards the mouth supplied by fluvial or diffusive processes. The greater the head value (value of h* at 0.2 a*), higher is the influence of diffusive processes in the development of fluvial landscape. A higher toe value (h* at 0.8 or 0.9 a*) represents, a greater extent of accumulation of materials (mass) derived from the head-ward portions of the basin. The toe value also underscores the degree of lateral drainage branching within the sub-basin (Willgooose and Hancock, 1998). Sub-basins 1, 4 and 5 are characterised by high toe values.

In CRB, width to length ratio of the drainage basin - the aspect ratio (*Bs*), ranges from 0.85 to 5.23 (Table 2). The *Bs* and h*(0.9) relation of the sub-basins are depicted in (Fig. 7a.). The average bifurcation ratio (Av: Rb) is directly proportional to the increment in *Bs* (Fig. 7b). The difference in toe height (h*0.8-h*0.9), (representing the rate of toe height increment) is determined, which is a measure of the volume of mass accumulation at mouth. Value of this parameter ranges from 0.1 - 0.02 and highest values are reported from sub-basins 4, 5 and 6. The relation between the rate of toe height increment and the aspect ratio (*Bs*) is shown in Fig. 7c.

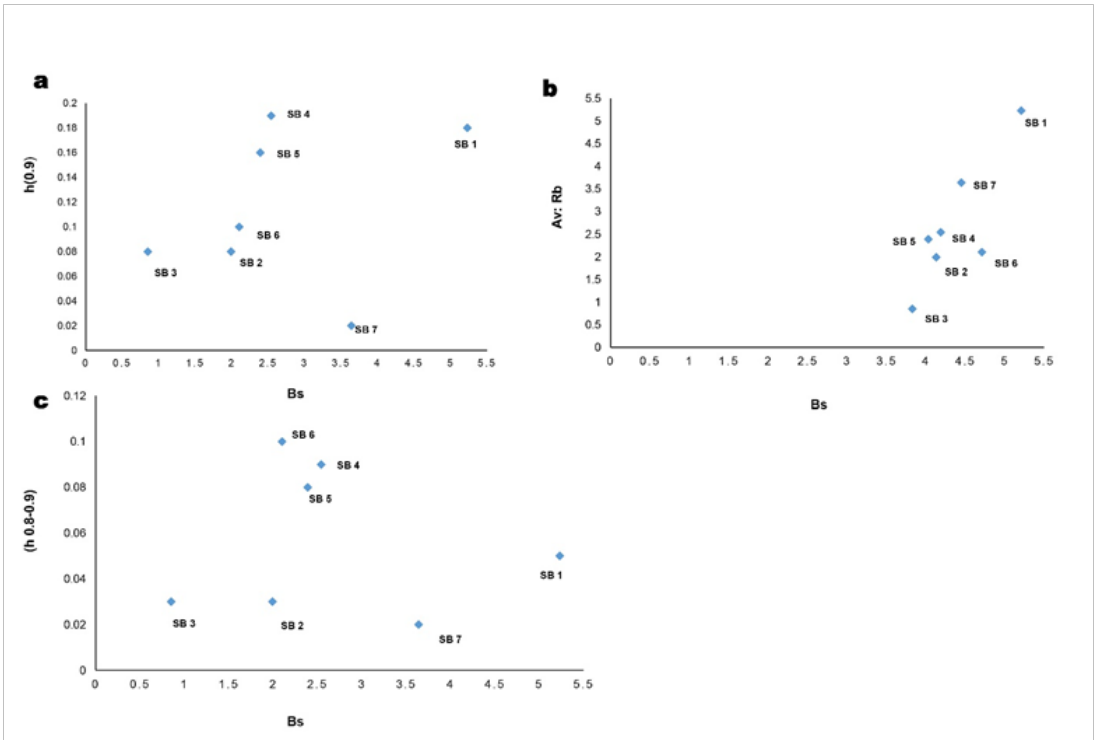

Figure 7 (a,b,c): Representation of the relation between *Bs-h*, Bs-h**0.8-*h**0.9 respectively

HYPSOMETRIC INTEGRAL (*Ea*) AND SLOPE INFLECTION POINT

Stages of geomorphic evolution can be interpreted from hypsometric integral. *Ea* values of the sub-basins of CRB are in the range of 0.41 to 0.48 (Table 4). The *Ea* of sub-basins are in the 0.35< *Ea* <0.6 class, which suggests the mature stage.

The hypsometric integral indicates the mass of land that resisted erosion. For instance, the sub-basin 5 with *Ea* value of 0.48, indicates that ~52% of the land had been eroded off, while 48% of land endured the process of erosion, and exhibits the mature stage of geomorphic evolution. The *HC* of the sub-basins falls under Type 4 standard curve, but not sub-basin 7.

Landform evolution model based on *Ea* and a* proposed by Sinha Roy (2002) is tested for CRB. The plot of *Ea* and a* usually shows two trends; decrease of *Ea* with decrease in a* (Model 1) and decrease of *Ea* with increase in a* (Model 2). Model 1 sub-basin is characteristic of Type 1 *HC* reflecting the dominance of fluvial process in landform evolution, whereas Model 2 sub-basins characterize Type 4 *HC*, representing initial process of fluvial process followed by diffusive processes. Sub-basin 7 belongs to Model 1 category and other sub-basins are classed as Model 2, which signifies that the drainage basin is evolved through initial fluvial and later diffusive process effected possibly through hill slope retreat (Fig.8). Pearson's correlation matrix analysis of the drainage morphometric parameters was carried out and are summarised in Table 5. Strong correlation between *Vf* and *T*, *Vf* and *Smf* was observed that implied erosional characteristics of the terrain and good correlation between *Ea* and *SL*, *Bs* and *SL* signified the erosional characteristics of the drainage basin. Strong negative correlation is observed between *Ea* and T.

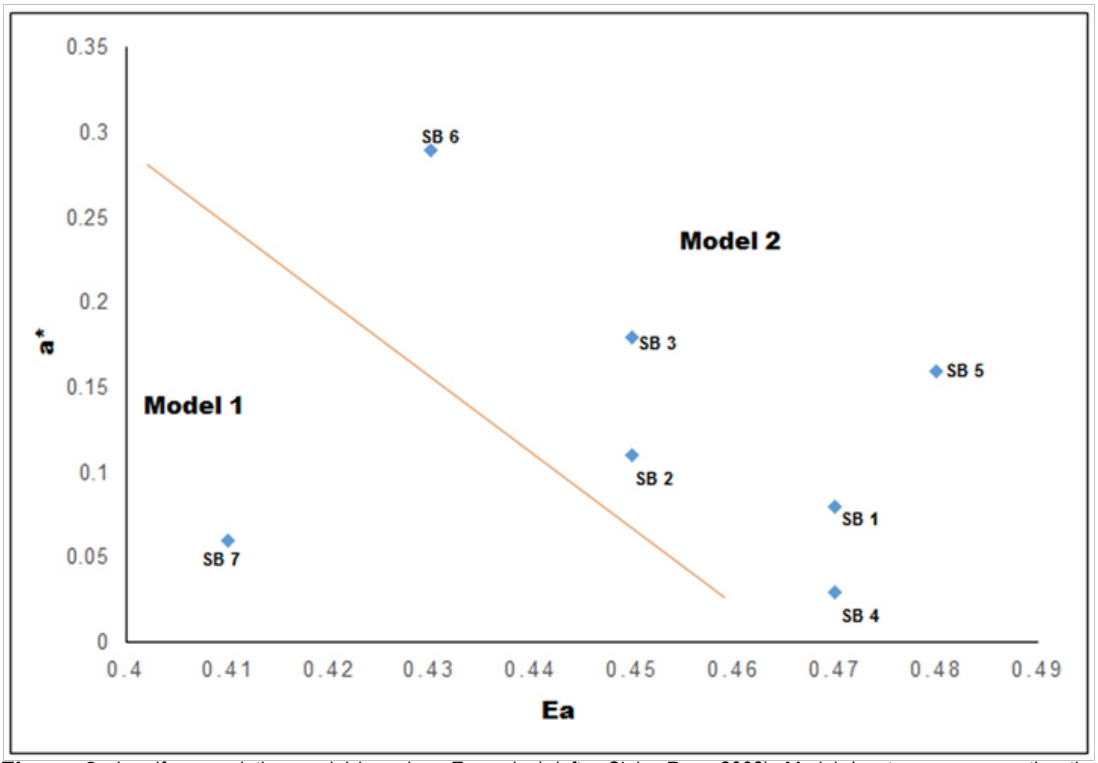

Figure 8: Landform evolution model based on Ea and a* (after Sinha Roy., 2002). Model 1 category representing the dominance of fluvial process in drainage basin evolution and Model 2 represents geomorphic evolution through initial fluvial erosion and later phase of diffusive processes.

Table 5: Pearson's correlation matrix of drainage morphometric parameters

	A	Ea	Bs	BAF	PBAF	T	SL	Vf	Smf	Av. Rb
A	1									
Ea	–0.54627	1								
Bs	0.37067	0.06132	1							
BAF	0.59452	0.15854	0.53994	1						
PBAF	–0.06008	–0.32065	0.5001	–0.17753	1					
T	0.7014	–0.93081	0.15259	0.05544	0.19854	1				
SL	0.03801	0.56683	0.57855	0.45153	0.27026	–0.54077	1			
Vf	0.56852	–0.66398	0.01454	0.36775	–0.15088	0.75636*	–0.54854	1		
Smf	0.40415	–0.5707	–0.59247	0.04304	–0.5285	0.55439	–0.74851	0.72832	1	
Av.Rb	0.61917	–0.35294	0.1982	–0.08704	–0.05652	0.39582	0.21623	–0.10338	0.10681	1

The study proposes that; albeit low-moderate tectonic imprints, diffusive processes/ fluvial erosion due to eustatic changes may have played a vital role in the evolution of geomorphological features in the CRB.

Conclusions

The trinity of lithology (structure), tectonics and climate, is in charge of development of a drainage basin that manifest as erosional process operating within it. The presence of charnockites, hornblende biotite gneiss, biotite gneiss, and intrusions of granites, syenites, and gabbro reveal the heterogeneity in the lithologic characteristics of CRB. The CRB is traversed by numerous prominent NNW-SSE trending structural lineaments along with sub-numerous NNE-SSW and E-W trending minor lineaments. The present study is carried out to interpret the processes involved in the drainage basin evolution and development. Basin asymmetry often reveals the role of tectonics in shaping the drainage basin characteristics. However, the morpho-tectonic interpretation form *Bs*, BAF, PBAF reveals symmetrical characteristics of CRB which in turn indicate moderate to low tectonic control in the drainage basin development. *Smf* values representing less active mountain fronts also substantiate the findings.

Hypsometric analysis is a chief vehicle in deciphering the geomorphic evolutionary stages, by piecing together data on the denudation status, geological processes ruling over the drainage basin development of CRB modeled from the study of sub-basins. Relative tectonic activity index (*Iat*) is high for sub-basin 1, while the other sub-basins show moderate to low tectonic response. Hypsometric curve shape of sub-basin 7 shows the dominance of fluvial processes in its evolution and other sub-basins of CRB are evolved through earlier stage of fluvial process and late-stage diffusive processes. The hypsometric integral value (*Ea*) representing extent of subdued topography is high for sub-basin 4. *Ea* value suggests that the sub-basins show mature stage of geomorphic evolution. CRB is evolved through earlier stage of fluvial process and late-stage diffusive processes. Recent landslides that have occurred in CRB as a consequence of climate changes can be connected to the basin's geomorphologic evolution.

Conflict of interest

On behalf of all authors, the corresponding author states that there is no conflict of interest.

Acknowledgements

The first author acknowledges sanctions from the University Grants Commission (UGC) New Delhi for conducting this research under Faculty Development Programme (XIIth plan). The author also expresses deep gratitude to the Principal, Government College Kottayam, for providing necessary facilities for doing this research.

References

Ahmad, S., Alam, A., Ahmad, B., Afzal, A., Bhat, M. I., Sultan Bhat, M., and Farooq Ahmad, H. (2018) Tectono-geomorphic indices of the Erin basin, NE Kashmir valley, India. *Journal of Asian Earth Sciences*, 151:16–30. https://doi.org/10.1016/j.jseaes.2017.10.013.

Ajayakumar, P.S., Rajendran., M. T. M. (2017) Geophysical lineaments of Western Ghats and adjoining coastal areas of central Kerala, southern India and their temporal development. *Geoscience Frontiers*, 8: 1089–1104.

Anderson, R. S, and Anderson, S. P, (2010) *Geomorphology: The Mechanics and Chemistry of Landscapes*. Cambridge University Press, 340 p.

Babu, K. J, Sreekumar, S, Aslam A. and Midhun, K. P. (2012) Hypsometry and Geomorphic Development of a Water shed : A Case Study

from South India. *International Journal of Science and Research*, 3(10): 1495–1500.

Bahrami, S, (2013). Analyzing the drainage system anomaly of Zagros basins: Implications for active tectonics. *Tectonophysics* 608: 914–928. http://dx.doi.org/10.1016/j.tecto.2013.07.026.

Bull, W. B, and McFadden, L. D. (1977) Tectonic geomorphology north and south of the Garlock fault, California. *Geomorphology in Arid Regions*, 115–138. papers3: //publication/uuid/30570AF0-83D9-4A20-A90B-A3EA72260B20.

Bull, W.B and McFadden, L.D, (1977) Tectonic geomorphology north and south of the Garlock fault, California. In: Geomorphology in Arid Regions. *Proceedings 8th Annual Geomorphology Symposiu*, State University New York at Binghamton, 115–138.

Chen, Y.C, Sung, Q and Cheng, K. Y. (2003) Along Strike Variations of Morphotectonic Features in the Western Foothills of Taiwan: Tectonic Implications Based on Stream-Gradient and Hypsometric Analysis. *Geomorphology,* 56, 109–137. https:// doi.org/http:// dx.doi.org/.10.1016/.S0169-555X (03) 00059-X.

Cox, R. T. (1994) Analysis of drainage-basin symmetry as a rapid technique to identify areas of possible Quaternary tilt-block tectonics: an example from the Mississippi Embayment. *Geological Society of America Bulletin.* https:// doi.org/ 10.1130/0016-7606 (1994) 106<0571:AODBSA>2.3.CO; 2.

Dar, R.A, Chandra, R, and Romshoo, S.A. (2013) Morphotectonic and lithostratigraphic analysis of intermontane Karewa Basin of Kashmir Himalayas, India. *Journal of Mountain Science*, 10(1), 1–15. https://doi.org/10.1007/s11629-013-2494-y.

Dash, P, Aggarwal, S.P, Verma, N, and Ghosh, S. (2014) Investigation of scale dependence and geomorphic stages of evolution through hypsometric analysis: a case study of Sirsa basin, western Himalaya, India. *Geocarto International,* 29(7): 758–777. https:// doi.org/ 10.1080/ 10106049.2013.841772.

Deffontaines, B, Chotin, P, Ait, Brahim, L. and R. (1992) Investigation of Active Faults in Morocco Using Morphometric Methods and Drainage Pattern Analysis. *Geologische Rundschau*, 81, 199–210.

Dehbozorgi, M, Pourkermani, M, Arian, M, Matkan, A.A, Motamedi, H. and Hosseiniasl, A. (2010) Quantitative analysis of relative tectonic activity in the Sarvestan area, central Zagros, Iran. *Geomorphology,* 121(3–4), 329–341. https://doi.org/10.1016/j.geomorph.2010.05.002.

Doranti-Tiritan, C, Hackspacher, P.C, Henrique De Souza, D, and Siqueira-Ribeiro, C. (2014) The Use of the Stream Length-Gradient Index in Morphotectonic Analysis of Drainage Basins in Poços de Caldas Plateau, SE Brazil. *International Journal of Geosciences*. https://doi.org/10.4236/ijg.2014.511112.

Duvall A.E. and Kirby, D.B. (2004) Tectonic and lithologic controls on bedrock channel profiles and processes in coastal California. *Journal of Geophysical Research*. 109. doi:10.1029/2003JF00086,2004.

El Hamdouni, R, Irigaray, C, Fernández, T, Chacón, J. and Keller, E. A. (2008) Assessment of relative active tectonics, southwest border of the Sierra Nevada (southern Spain). *Geomorphology*, 96(1–2): 150–173. https://doi.org/10.1016/j.geomorph.2007.08.004.

Fairbridge, R. (1968) Terraces, fluvial-environmental controls. *Encyclopedia of Geomorphology*, Reinhold, New York, 1124–1138.

Farhan, Y, Elgaziri, A, Elmaji, I, Ali, I, and Farhan, Y. (2016) Hypsometric Analysis of Wadi Mujib-Wala Watershed (Southern Jordan) Using Remote Sensing and GIS Techniques. *International Journal of Geosciences*. https://doi.org/10.4236/ijg.2016.72013

Gadre, R J, (2006) *River Morphology*. New International Publishers, Delhi. 479p.

Hack, J.T. (1973) Stream Profile Analysis and Stream Gradient Index. *U.S. Geological Survey*. J 1(4): 421–29.

Hare, P.W. and Gardner, T.W. (1985) Geomorphic Indicators of Vertical Neotectonism along Converging Plate Margins, Nicoya Peninsula Costa Rica. In Morisawa, M. and Hack, J.T. (Eds.), *Tectonic Geomorphology*.

Proceedings of the 15th Annual Binghamton Geomorphology Symposium, Allen and Unwin, Boston: 123–134.

Kale, V.S. and Gupta, A. (2001) *Introduction to Geomorphology*. Orient Longman, New Delhi: 278p.

Keller, E.A, and Pinter, N. (1996) *Active Tectonics: Earthquakes, Uplift, and Landscape*. Prentice Hall, Upper Saddle River, 338p.

Lavé, J, and Burbank, D. (2004) Denudation processes and rates in the Transverse Ranges, southern California: Erosional response of a transitional landscape to external and anthropogenic forcing. *Journal of Geophysical Research*: Earth Surface. https://doi.org/10.1029/2003JF000023

Lifton, N.A. and Chase, C.G, (1992) Tectonic, Climatic and Lithological Influences on Landscape Fractal Dimensions and Hypsometry: Implications of Landscape Evolution in the San Gabriel Mountains, California. *Geomorphology*, 5: 77–114.

Mahmood, S. A, and Gloaguen, R. (2012) Appraisal of active tectonics in Hindu Kush: Insights from DEM derived geomorphic indices and drainage analysis. Geoscience *Frontiers,* 3(4): 407–428. https://doi.org/10.1016/j.gsf.2011.12.002

Martinez, M, Hayakawa, E.H, Stevaux, J.C, Profeta, J.D. (2011) SL Index as indicator of anomalies in the longitudinal profile of the longitudinal profile of Pirap´o river, S̃ao Paulo, UNESP, *Geosciences*, 30:.63–76.

Ouchi, S, (1985) Response of alluvial rivers to slow active tectonic movement, *Geological Society of America Bulletin,* 96: 504–515.

Özkaymak, Ç, and Sözbilir, H. (2012) Tectonic geomorphology of the Spildağı High Ranges, western Anatolia. *Geomorphology*, 173–174 (January): 128–140. https:// doi.org/ 10.1016/j.geomorph.2012.06.003.

Panek, T. (2004) The Use of Morphometric Parameters in Tectonics Geomorphology (on the Example of the Western Beskydy MTS). *Journal of Geographia*, 1: 111–126.

Pérez-Peña, J.V, Azañón, J.M, Azor, A, Delgado, J, González-Lodeiro, F, (2009) Spatial analysis of stream power using GIS: SLk anomaly maps. *Earth Surface Process and Landforms.* 34: 16–25.

Pike, R.J. and Wilson, S.E. (1971) Elevation-Relief Ratio, Hypsometric Integral and Geomorphic Area-Altitude Analysis. *Geological Society of America Bulletin*, 82: 1079–1084. http://dx.doi.org/10.1130/0016-7606 (1971) 82 [1079:ERHIAG] 2.0.CO;2.

Schumm, S.A. (1956) Evolution of Drainage Systems and Slopes in Badlands at Perth Amboy, New Jersey. *Geological Society of America Bulletin*, 67: 597–646. http:// dx.doi.org/ 10.1130/ 0016-7606 (1956)67[597:eodsas] 2.0.co; 2.

Sedrette, S, Rebaï, N, and Mastere, M. (2016) Evaluation of Neotectonic Signature Using Morphometric Indicators: Case Study in Nefza, North-West of Tunisia. *Journal of Geographic Information System,* 8: 338–350. https://doi.org/10.4236/jgis.2016.83029

Singh, Yogendra, Biju John, G. P. Ganapathy, Abhilash George, S. Harisanth, K. S. Divyalakshmi, and Sreekumari Kesavan. (2016) Geomorphic Observations from Southwestern Terminus of Palghat Gap, South India and their Tectonic Implications. *Journal of Earth System Science*, 125(4): 821–39. https://doi.org/10.1007/s12040-016-0695-9.

Sinha Roy S, (2002) Hypsometry and landform evaluation: a case study in Banas drainage basin, Rajasthan, with implications for Aravalli uplift. *Journal of the Geological Society of India*, 60:7–26.

Soman, K. (2002) *Geology of Kerala.* Geological Society of India, Bangalore. viii, 335 pages

Strahler, A. (1964) Quantitative Geomorphology of Drainage Basins and Channel Networks. In: Chow, V, Ed, *Handbook of Applied Hydrology,* McGraw Hill, New York, 439–476.

Strahler, A.N. (1952a) Hypsometric (Area-Altitude) Analysis of Erosional Topography. *Geological Society of America Bulletin*, 63: 1117–1142.

Strahler, A.N. (1956b) Quantitative slope analysis. *Geological Society of America Bulletin,* 11: 1117-1142 https:// doi.org

10.1130/0016-7606(1952)63[1117:HAAOET]2.0.CO;2

Strahler, A.N. (1957) Quantitative analysis of watershed geomorphology. Eos, *Transactions American Geophysical Union*. 38(6): 913–920. https://doi.org/10.1029/TR038i006p00913

Thomas, J, and Prasannakumar, V. (2017) Implications of shearing on drainage network development in Achankovil Shear Zone, South India: insights from DEM-based geomorphic indices and longitudinal profile analysis. *Environmental Earth Sciences*, 76(20): 1–21. https://doi.org/10.1007/s12665-017-7016-8

Troeh, F.R. (1965) Landform equations fitted to contour maps. *American Journal of Science.* https://doi.org/10.2475/ajs.263.7.616

Walcott, R.C. and Summerfield, M.A. (2008) Scale dependence of hypsometric integrals: An analysis of southeast African basins. *Geomorphology*, 96: 174–186. https:// doi.org/ 10.1016/j.geomorph.2007.08.001.

Willett, S.D., McCoy, S.W., Taylor Perron, J, Goren, L. and Chen, C.Y. (2014) Dynamic reorganization of River Basins. *Science*, 343: 6175. https://doi.org/10.1126/science.1248765

Willgoose, G, Bras, R.L, and Rodriguez Iturbe, I. (1991) A physical explanation of an observed link area-slope relationship. *Water Resource Research*, 27(7): 1697–1702. https:// doi.org/ 10.1029/ 91WR00937

Willgoose, G, (1994) A statistic for testing the elevation characteristics of landscape simulation models. *Journal of Geophysical Research:* Solid Earth, 99(B7): 13,987–13,996. 99-B7.13,987-13,996.

Willgoose, C, Hancock, G, (1998) Revisiting the hypsometric curve as an indicator of form and process in transport-limited catchment. *Earth Surface Processes and Landforms*. 23: 611–623. http:// dx.doi.org / 10.1002 / (SICI)1096-9837(199807)23:7<611::AID-ESP872>3.0.CO,2Y

Date received: 31.7.2021

Date accepted after revision: 8.11.21